Journal of Applied Polymer Science

Multilayer photoactive nanocolloidal PPy:PSS as a novel substitute for Pt free counter electrode in DSSC

S. Maruthamuthu,[1,2] J. Chandrasekaran,[3] D. Manoharan,[3] S. N. Karthick,[4] Hee-Je Kim[4]

[1]Research and Development Centre, Bharathiar University, Coimbatore, Tamil Nadu, 641 046, India
[2]Faculty of Physics, Dr. Mahalingam College of Engineering and Technology, Pollachi, Tamil Nadu, 642 003, India
[3]Department of Physics, Sri Ramakrishna Mission Vidyalaya College of Arts and Science, Coimbatore, Tamil Nadu, 641 020, India
[4]School of Electrical Engineering, Pusan National University, Busan, 609 735, Republic of Korea
Correspondence to: S. Maruthamuthu; (E-mail: smaruthamuthu@gmail.com)

ABSTRACT: Water dispersible and highly processable, Polypyrrole (PPy) nanocolloidal particles were synthesized by chemical oxidation polymerization with 15 wt % of anionic polyelectrolyte poly(styrene sulfonate) (PSS) at 5°C has been reported in this work. This polymer composite (PPy:PSS) was competent with conventional Pt counter electrode (CE) when compared for dye sensitized solar cells (DSSCs). Morphological analysis revealed smooth and spherical shaped nanoparticles of PPy. Interaction between the SO_3H groups and Py units in PPy improved the thermal stability of PPy with higher doping levels of PSS. The nanocolloidal solution was spin coated at 4000 rpm. The layer by layer, self-assembled multilayer thin films were used as CE in DSSCs. There was a linear dependence of DSSCs performance with film roughness for the self-assembled multilayer PPy:PSS films. Single layer films showed better electrocatalytic behavior than multilayer films. All the PPy:PSS films had good electrochemical stability. The DSSC efficiency of 3.40% was observed for chemically oxidized PPy with 15 wt % PSS for single layer film, with a highest FF of 0.7154. The low cost, good performance, rapid and simple fabrication method of PPy:PSS composite modified CE could be a potential alternative for Pt in the DSSCs. © 2015 Wiley Periodicals, Inc. J. Appl. Polym. Sci. **2016**, *133*, 43114.

KEYWORDS: conducting polymers; morphology; nanostructured polymers; self-assembly; thermogravimetric analysis

Received 1 May 2015; accepted 31 October 2015
DOI: 10.1002/app.43114

INTRODUCTION

Dye-sensitized solar cells (DSSCs), a third generation solar cell is a vital device to develop sustainable energy.[1] It has the promising potential to produce electricity from solar energy efficiently.[2] Simple fabrication and controllable redox properties of DSSCs with better flexibility have attracted scientists more than a decade.[3] A typical DSSCs comprises of a high surface area of dye sensitized TiO_2 porous film on a piece of transparent conducting oxide glass that acts as photo anode, a good ion-transporting electrolyte containing a redox couple ($\bar{I}/I_3$) and an efficient counter electrode.[4] Counter electrode (CE) plays a key role in the performance of DSSCs because it serves as a mediator for collecting electrons from external circuit and reduces I_3 ions to $\bar{I}$ ions, thus regenerating the oxidized dye after electron injection. An efficient CE can reduce internal energy loss in DSSCs and produce higher current densities and fill factors.[5] So far, Pt CE remains the stalwart due to its high catalytic activity and low charge transfer resistance. However, high cost and limited availability of Pt is a significant setback for the mass production of DSSCs. Moreover, the dissolution of Pt in $\bar{I}/I_3$ electrolyte reduces the long term stability of DSSCs.[6] Thus alternative materials for Pt free CE with low cost and corrosion resistance with good conversion efficiencies have been developed mainly with carbon-based materials,[7,8] transition metal based inorganic materials[9,10] and bimetallic oxides.[11,12] Interestingly, organic conducting polymers such as polyaniline, polypyrrole, poly(3,4 ethylenedioxythiophene) are recently been another promising alternatives. Their derivatives are preferred for their high conductivity, diverse structure, good chemical stability with electrocatalytic activity, ready synthesis, low cost, non-toxicity and large scale (flexible) device fabrication.[13–15] However, since certain conducting polymers are very expensive and can only be electrodeposited within a limited area of electrode, the production cost can increase more than using Pt as CE. PPy has been widely studied in various applications including super-capacitor, sensor, field emission, secondary battery electrode and metal anti-corrosion materials and so on.[16,17] PPy can be easily

Additional Supporting Information may be found in the online version of this article.

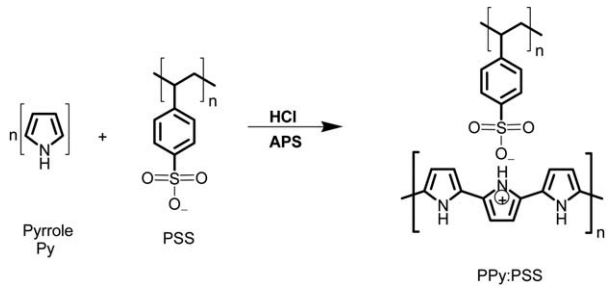

Scheme 1. The synthetic procedure of the formation of water-dispersible PPy:PSS

prepared by chemical oxidation and electrochemical polymerization of pyrrole monomer. Although the latter has the advantage of controllable initiation and termination of polymerization, easy and *in situ* polymerization at low temperature,[18] it is not suitable for mass production. In contrast, chemical oxidative polymerization is simple, cheap, and fast which can be scaled up, but in either case PPy exhibits poor solubility. This could be improved by designing colloidal form of PPy using surfactants and polymeric stabilizers.[19] Incorporation of anionic surfactant with PPy as dopant would enhance the physical properties of PPy.[20] Nanoparticles of PPy, prepared by chemical polymerization was used as CE in DSSCs by Wu *et al.*[21] and PPy nanospheres by Jeon *et al.*[22] and they have obtained high DSSCs efficiency. Many oxidants such as $FeCl_3$, ferric perchlorate and ammonium peroxydisulfate (APS) with various additives along with the synthesis condition could affect the properties of the fabricated conducting polymers in this chemical process.[23,24] Qi and Pickup[25] showed the presence of (PSS) in the reaction medium that allows the size of chemically synthesized PPy:PSS particles to be controlled by varying the concentration of the oxidant. Particle sizes thus obtained range from about 40 nm to 1 μm. Poly (styrene sulfonate) can be immobilized in a polymer matrix due to its large size, and would show good exchange properties during the redox process, thus providing higher capacity and better diffusion of ionic species of PPy.[26] In this article, we have reported a simple chemical oxidative polymerization of PPy nanocolloidal particles along with milder oxidant (APS) in the presence of 15 wt % of PSS, which is a typical polymeric surfactant used as dopant for polymerization. The PPy that, showed good water dispersible nature and enhanced processability was spin-coated on Fluorine doped tin oxide (FTO) at 4000 rpm and multilayer (1, 3, and 5) thin films were prepared and used as CE in DSSCs. The performance was analyzed relative to the Pt CE and the morphological variation of PPy in the presence of higher wt % of PSS and its influence in multilayer CE were discussed. The molecular structures of the molecules used for the formation of the water dispersible nanocomposite are shown in the Scheme 1.

MATERIALS AND METHODS

Preparation of PPy:PSS Nanocolloidal Particles and Multilayer Thin Films

The nanocolloidal polypyrrole was chemically synthesized by oxidative polymerization using APS $(NH_4)_2S_2O_8$ as oxidant in the presence of HCl and PSS. In this typical synthesis, 15 wt % of PSS (corresponds to monomers weight) was dissolved in 90 mL of 1.0 M aqueous HCl solution in a reaction vessel and the pyrrole monomer (0.67098 g) was mixed with the solution drop by drop. Pyrrole was dissolved thoroughly in the aqueous solution of combined primary dopant HCl and secondary dopant PSS with the aid of ultrasonication. An amount of 10 mmol (2.28 g) APS was dissolved in 10 mL of deionized water with the help of ultrasonication and then slowly added into the solution of monomers with HCl and PSS dopants. The polymerization was carried out for 24 h at 5°C with constant mechanical stirring. The stable black colored PPy:PSS nanocolloidal dispersion was obtained after the polymerization as shown in the Scheme 2. The resulted PPy:PSS solution was spin coated on FTO glass with sheet resistance 13 Ω/sq, (Hartford glass co.inc) for thin films with different number of layers (1, 3, and 5). Before the film formation, FTO substrates were cleaned with detergent, triple distilled water, acetone and isopropyl alcohol and dried by a hot air dryer. All the substrates were preheated at 90°C over a hotplate for 3min to remove the moisture and PPy:PSS solution was then, coated with typical spin speed of 4000 rpm for 30 s. Each layer produced by spin coat was post-heated at 120°C for 3 min and finally dried at 120°C for 30 min.

Fabrication of DSSCs

An FTO glass, which was used as a current collector with resistance of 13 Ω/sq was first cleaned for 10 min each in acetone, ethanol and water through ultrasonic bath. To control the film thickness scotch tape was used as a spacer and it also created a non-coating area for electrical contact. TiO_2 (Ti-Nano oxide T/Sp, Solaronix) paste was coated on an FTO plate by doctor blade method and was used as photoanode. To reduce the surface irregularities of TiO_2 films thus coated were air dried for 5 min. Films were annealed at 450°C in air for 30 min to remove the organic loads, and it facilitated the interconnection of TiO_2 nanoparticles. The photoanode thus prepared had a thickness of 20 μm with an active area of 0.20 cm^2. After cooling down to 75°C, the TiO_2 film electrodes were immersed in a 0.3 m*M* N719 dye solution for 24 h. After dye adsorption, the film was

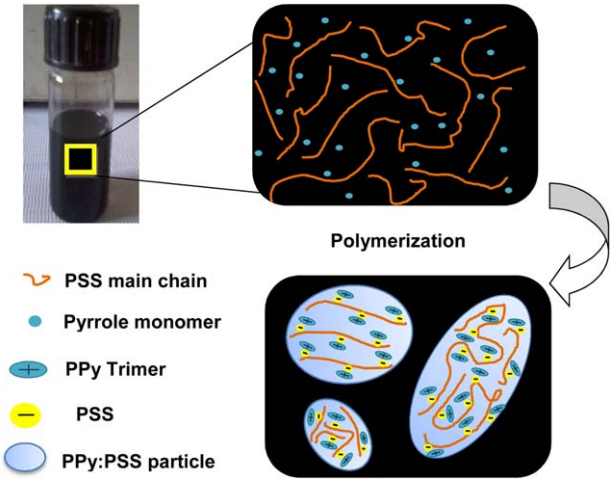

Scheme 2. Effect of PSS and its negatively charged groups water dispersed polypyrrole nanocolloidal particles. [Color figure can be viewed in the online issue, which is available at wileyonlinelibrary.com.]

rinsed with pure ethanol to remove the excess dye and dried with hot air. The Pt electrode was prepared from Pt paste (Plastisol T/sp, Solaronix) by doctor blade method. After coating on a FTO plate, it was annealed at 450°C for 30 min. The dye covered TiO_2 photoanode and the PPy:PSS multilayer (1, 3, and 5) coated counter electrodes were assembled as a sandwich type, using a thermoplastic hot-melt ionomer film (SX 1170, Solaronix). The active cell area used was 0.25 cm^2. A drop of an Iodolyte AN-50 electrolyte solution was injected in to the cell through a hole at the back of the CE. The hole was covered with a cover glass on a hot-melt ionomer film and then sealed. Finally, the edge of each side of the FTO glass was cleaned and soldered (Ultrasonic soldering system, Model-9200) with alloy # 143 (Cerasolza) to achieve good electrical contact for the measurements.

Characterization Techniques

The water dispersible PPy:PSS nanoparticles have been precipitated with excess of ethanol in order to obtain the solid form of PPy:PSS nanoparticles. The precipitated particles were dried at 60°C in vacuum for 24h. The Fourier transform infrared spectroscopy (FT-IR) spectrum of the sample in KBr pellet was obtained using a (Bruker IFS 66 V) IR spectrophotometer. The UV–visible spectrum of PPy:PSS solution was obtained by (Perkin-Elmer Lambda 35) UV–vis spectrometer. The particle size distribution of PPy:PSS solution was determined by laser light scattering with a (Zetasizer) particle size analyzer, Malvern, UK. The suspension was diluted to the appropriate concentration with double-distilled water before the measurement. Transmission electron microscopy (TEM) observation was performed using a (EOL-1200 EX) transmission emission microscope operated at a 100 kV accelerating voltage in which specimens were prepared by spreading a small drop of the sample solution on a 400 mesh copper grid. The PPy:PSS nanocolloidal solution was diluted in two ways, one by using ethanol and another by using water for TEM analysis. Electrochemical impedance spectroscopy (EIS) was performed using a BioLogic potentiostat/galvanostat/EIS analyzer (SP-150, France) under 1 sun illumination. The surface roughness and topology of the PPy:PSS films were analyzed by atomic force microscopy (AFM, model: Solver Pro M of NT-MDT working in semi-contact mode). The elemental analysis of PPy compositions with higher wt % of PSS were performed by using Thermofinnigan (FLASH EA 1112). The stability of the PPy was studied with (DuPont TA Instrument 2050) Thermogravimetric analyzer at a heating rate of 20°C/min under nitrogen atmosphere using platinum pans from 30 to 800°C. The cyclic voltammetry (CV) measurements were carried out on a CHI 660 C electrochemical workstation (CH instruments) using three electrode set up with PPy:PSS as working electrode, platinum wire as counter electrode and an Ag/AgCl as reference electrode. The active material PPy:PSS was spin coated at 4000 rpm over ultrasonically cleaned FTO glass substrate with an area of 1×1 cm^2 was used as a working electrode. The CV curves were recorded between −0.2 and 1 V as potential window and 0.1M H_2SO_4 was used as electrolyte solution. The current-voltage characteristics were measured at one sun illumination (AM 1.5G, 100 $mWcm^{-2}$) using a solar simulator (SAN-EI Electric XES-301 S 300W Xe Lamp). Keithley 2400 was used as the source measurement unit. The photoelectric conversion efficiency (η) was calculated using the following eq. (1).

$$\eta\,(\%) = \frac{V_{oc} \times I_{sc} \times FF}{P_{in}} \times 100 \quad (1)$$

Where η is the global efficiency, V_{oc}, I_{sc}, and FF are open circuit voltage, short circuit current and fill factor, respectively, and P_{in} is the maximum input of light energy (100 $mWcm^{-2}$).

RESULTS AND DISCUSSION

UV-Vis Absorption Spectra

The interfacial interaction of PPy and PSS and the uniformity of the films were analyzed using UV-Vis spectroscopy. Supporting Information Figure S1 shows the UV-Vis absorption spectrum of PPy:PSS multilayer films. The absorption is seen over a broad wavelength range for all the multilayer films, which is suitable for photovoltaic applications. A typical absorption peak occurs at 585 nm for 1, 3, and 5 layers of PPy:PSS films which is due to π-π^* transition, and is closely related to the counter anions doped in PPy chains.[18] Then, the band ranging up to 1000 nm corresponds to the band gap energy between the valance band and bipolaron band of the conjugated PPy, which can be related to the conjugation length of doped PPy and also to that of antibipolarons of the oxidized form of PPy.[27,28] Due to the presence of higher wt % of PSS, the structure of PPy was continuously doped. The absorption peak associated with the polaron-π transition was significantly shifted to a smaller wavelength with the increasing PSS content,[29] and so there might be a possible interaction between the quinoid rings of PPy and SO_4^{2-} ion of PSS. The conductivity of PPy and its doping state can be altered by the presence of PSS. Thus the UV-Vis spectra reveal a slightly higher absorption magnitude for the multilayer films and show no influence of the position of the absorption maxima.

Elemental Analysis

The elementary composition (mass percent) of C, N, O, and S for the synthesized polypyrrole without dopant and two dopants (HCl as primary and PSS as secondary) were summarized in Table I. For three pyrrole rings, one positive charge is created and anions of the oxidant molecules will balance them.[30] The elemental content was calculated based on this assumption. The C/N ratio from Table I was in good agreement between PPy-SO_4. When APS was added in the synthesis, the SO_4^{2-} anion was able to compensate the positive charge of six pyrrole rings. The doping level for one PPy ring in PPy chain is represented by the N/S ratio.[31] From the experimental data, it is calculated that the fabricated PPy had a doping level of eight pyrrole rings for one dopant. When 15 wt % of PSS was added in the synthesis, the experimental N/S molar ratio decreased to 1.54 from 7.56 (for undoped PPy). This was due to the presence of higher wt % of PSS in the synthesis. It was also an indication, that PPy was doped with PSS. Table I clearly shows the increase in the S/N ratio when 15 wt % of PSS is added in the synthesis. This is a sign of PPy with high doping level, when the PSS content increased.[32] Increase in the sulfur amount also indicates that, some sulphate anions have been retained from reduction of persulfate oxidant and they are almost certainly doped in to the polypyrrole polymers.[30] From the samples synthesized in the

Table I. Elemental Analysis of PPy Synthesized without and with 15 wt % of PSS

Sample	C	N	S	H	C/N	C/H	N/S	S/N
PPy:PSS 1:0	48.59	14.21	4.3	2.47	3.99	1.65	7.56	0.13
PPy:PSS 1:15	27.95	8.00	11.92	4.98	4.07	0.47	1.54	0.65

presence of HCl and PSS, there was a fraction of higher H, compared to the results of elemental analysis of pure PPy, but the content of N was lower. This was caused by the presence of aliphatic or aromatic chains of surfactants in PPy.[32] The quantity of PPy in the presence of oxidant and anionic surfactant was higher when compared to the yield of PPy when using only APS, although same amount of oxidant was used in both the polymerization processes. These results indicate that, the part of anionic surfactant can be incorporated in to the PPy structure, similar to the anion of oxidant.

FTIR

Figure 1 shows the FTIR spectra of PPy that was fabricated with 15 wt % of PSS which exhibits all characteristic vibrations of PPy. A weak absorption band at 1640 cm^{-1} was due to the hydrated water molecules associated with PSS group via hydrogen bonding.[33] The peaks at 1403 cm^{-1} and 1313 cm^{-1} were due to the ring stretching vibrations and deforming vibrations of C—H and N—H. The absorption peaks at 1190 and 935 cm^{-1} represent the doping state of PPy. For undoped PPy a self-protonation of polymer occurs due to the sulfuric acid which is produced by the decomposition of peroxydisulfate, hence the similar peaks appeared for them as well. The lower absorption at 640 cm^{-1} was due to C—H out of plane bending of pyrrole moiety in PPy.[21] The peaks at 2998 and 2839 cm^{-1} originated due to the asymmetrical and symmetrical stretching of CH_2 group.

TGA

Figure 2 shows the TGA curves of weight loss, versus temperature for PPy synthesized with 15 wt % of PSS and pure PPy. Due to the hygroscopic character of PPy, an initial weight loss occurred significantly at 100°C for pure polypyrrole and at this temperature, the residual water evaporated. Moreover, it's worth mentioning here that at this temperature the weight loss of PPy, fabricated with 15 wt % of PSS is very low. These results indicate the improved stability of PPy synthesized with 15 wt % of PSS as regards affinity to water. With further increase in temperature at about 200°C, there occurred a main mass loss in doped PPy, which was an indication of polymer degradation and it was slightly lesser than the undoped PPy. This was because of, the decomposition of PPy which occurs initially along with the elimination of sulfonic acid groups.[33] The interaction doping between the SO_3H groups and Py units in polypyrrole could retard the sulfonic acid groups elimination. With more number of doping pairs, the sample will be more thermostable.[33] In general, free sulfonate groups are thermally active and they could possibly weaken the thermal degradation of PPy composite. The acidity also increased with the presence of 15 wt % of PSS, which accelerated the polymerization rate and could produce some defects in the PPy:PSS chains.[26] However, the sulfonate group became much more thermally stable when it formed a complex with countercation. These results indicate, that by introducing 15 wt % of PSS in the PPy system, the thermal stability of PPy could be effectively enhanced and create better interaction between PSS and PPy in the sample.

Particle Size

The particle size of PPy could be controlled by PSS, in which the anionic electrolyte can be incorporated in the PPy mesostructure which will serve as a dopant. The presence of higher wt % of PSS will play dual roles, one as an active participant as counterion to PPy and other as a surfactant in the polymerization.[31] It is well established that surfactants assemble in to

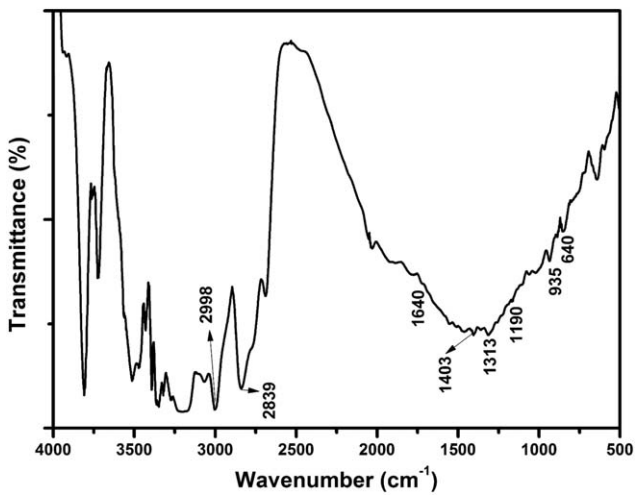

Figure 1. FTIR Spectra of PPy:PSS composite.

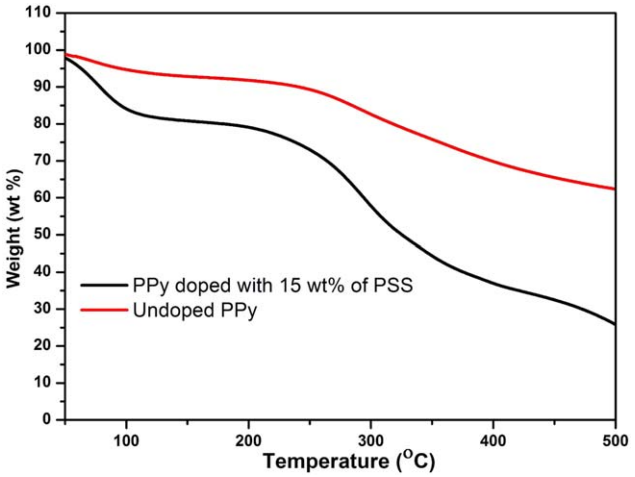

Figure 2. TGA data for PPy synthesized with 15 wt % of PSS/Pyrrole monomer. [Color figure can be viewed in the online issue, which is available at wileyonlinelibrary.com.]

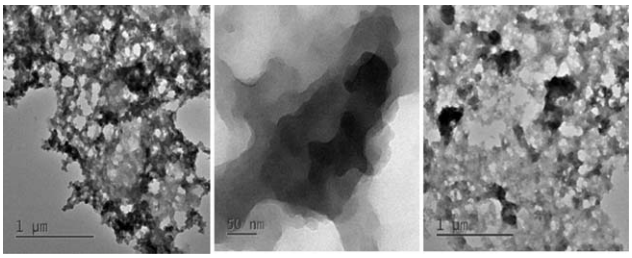

Figure 3. HRTEM images of water dispersed PPy:PSS composites.

micelles or spherical structures due to their amphiphilic nature in aqueous solution above a critical concentration. At relatively low reaction temperature, the mobility of higher concentration of surfactant is restricted by reducing the inner volume of the micelles, which encapsulate the monomer and oxidant. Because the interior volume of micelles is a function of surfactant concentration, the reduced micelle volume results in the decreased nanoparticle size of PPy. The size of PPy nanoparticles synthesized in the presence of 15 wt % of PSS at 5°C was around 500 nm, which indicates that, the particle size and morphology of PPy depends on the concentration of the surfactant. Likewise, the grain size of PPy synthesized by Wu *et al.*[21] (40–60 nm), Jeon *et al.*[22] (85 nm) and Qi *et al.*[25] (40–850 nm) were different, which depends on the concentration of monomer, oxidant and also on the synthesis condition. In our case anions of the oxidizing agents have played a different role of counterions in altering the ion pair interaction and in turn, the growth of PPy nanostructure may be confined in different ways during polymerization. This proves a potential route for the variable size of PPy particles in which no regular nanostructure of PPy was observed from particle size analyzer. Anionic surfactants would also serve as counterions for the polymer chains, and thus permanently disrupt the structure of the sphere like micelles.[34] Hence, the surfactants and oxidizing agents that are used have played a key role in tailoring the resultant conducting PPy nanostructures. When ionic oxidizing agent is added into the solution, it gradually diffused in to the Py reservoir and then oxopolymerize the Py monomers in to Polymers. Finally, the sphere like PPy nanostructures was obtained as a consequence of spatially constraint sphere like micelles.[34] The morphology of PPy:PSS nanostructures greatly depend on monomer concentration, surfactant concentration and surfactant chain length, which would provide the possibility of elaborate control of the morphologies of the resulting conducting polymer.[35]

HRTEM

Figure 3 shows the High-resolution transmission electron microscopy (HRTEM) images of PPy with 15 wt % of PSS, which serves as micelles for the formation of spherical shaped particles. The sample seems to have formed clusters of jumbled particles with uniform solid nanoparticles. It is necessary to point out that the synthesis of PPy:PSS composites with 15 wt % of PSS is a size-controllable process, which strongly depends on the content of PSS.[25] The elemental analysis reveal that PPy:PSS composites with higher wt % of anionic polyelectrolyte has lower polaron mobility, which is due to the enhanced hydrogen bond between PPy and PSS.[29] Hence, these particles have been homogeneously dispersed in the Py monomer to a uniform layer. Thus when spin-coated, it is expected to possess a higher effective surface area and larger rough surfaces that are vital for a counter electrode.

Surface Morphology of Multilayer Films

The surface morphologies of spin coated PPy:PSS multilayer films were investigated by AFM and the results are shown in Figure 4(a–c). The rate of coverage of the 1, 3, and 5 multilayer samples were obtained based on the height exclusion from the AFM images which looks linear for multilayer films. This is an indication that PPy:PSS is self-healing with respect to the addition of subsequent layers. There was also a significant improvement in the grain height, along with film thickness and grain size with the increase in the number of PPy:PSS layers. Though the thickness increment is the most straight forward parameter, the variation in grain size for multilayer films is due to the aggregation of PPy:PSS particle in a larger unit. Due to this particle aggregation, the surface roughness and root-mean-square (RMS) value of these thin films get enhanced. The aggregation of PPy:PSS particles will also facilitate higher surface area in the films which can possibly improve the tri-iodide diffusion efficiency[36,37] and generally, the evolution of film roughness is consistent with the film growth behavior. The roughness of the first bilayer was 18 nm and the films with 3 and 5 bilayers have roughness value of 65.9 and 83.03 nm, respectively. In Figure 4(a-c), the surface morphology showed many plate-like particles or aggregate of particles covering the surface, thus giving an increased surface roughness for the multilayer film. This is due to the tendency of PPy:PSS polyelectrolyte to be a colloidal dispersion in aqueous solution. Moreover, higher surface roughness leads to reduced optical transmittance in the UV-visible spectra, which is attributed to the scattering loss phenomenon.[38] Similarly, the RMS values of the multilayer thin films are 21, 82, and 98 nm for 1, 3, and 5 layer, respectively.

Multilayer PPy:PSS Films

PPy nanocolloidal particles were synthesized by adding 15 wt % of PSS gradually to the pyrrole monomer. Multilayer (1, 3, and 5) thin homogeneous films of PPy:PSS composites were obtained, by spin-coating the colloidal solution on the FTO glass substrates at 4000 rpm for 30 seconds. These multilayer thin films were annealed at 120°C for 30 min. The PSS chain segments will shrink after annealing, if the electrostatic coupling between PSS and the cation (like PPy) is not strong.[39] The accessibility of PSS to water molecules will be reduced due to this shrinking[40] and the reduced water sorption of the PSS-rich phase will then reduce the degree of relative humidity on the annealed PPy:PSS thin film.[41,42] Thus, thermally annealed PPy:PSS films exhibit stronger resistance to water absorption. Annealing will increase the interfacial adhesion of PPy:PSS on the substrate and thus reduce dewetting.[43] This can be also due to the higher surface energy of the discrete PPy nanoparticles. There will be an extended chain conformation of PPy with higher 15 wt % of PSS in water, and this is bound to happen as the conducting polymer in doping state is more rigid.[44] In the doped state this extended chain conformation is attributed to incorporating strands of the extended chain of PPy and PSS intertwined. When the aqueous solution of PPy:PSS was spin-

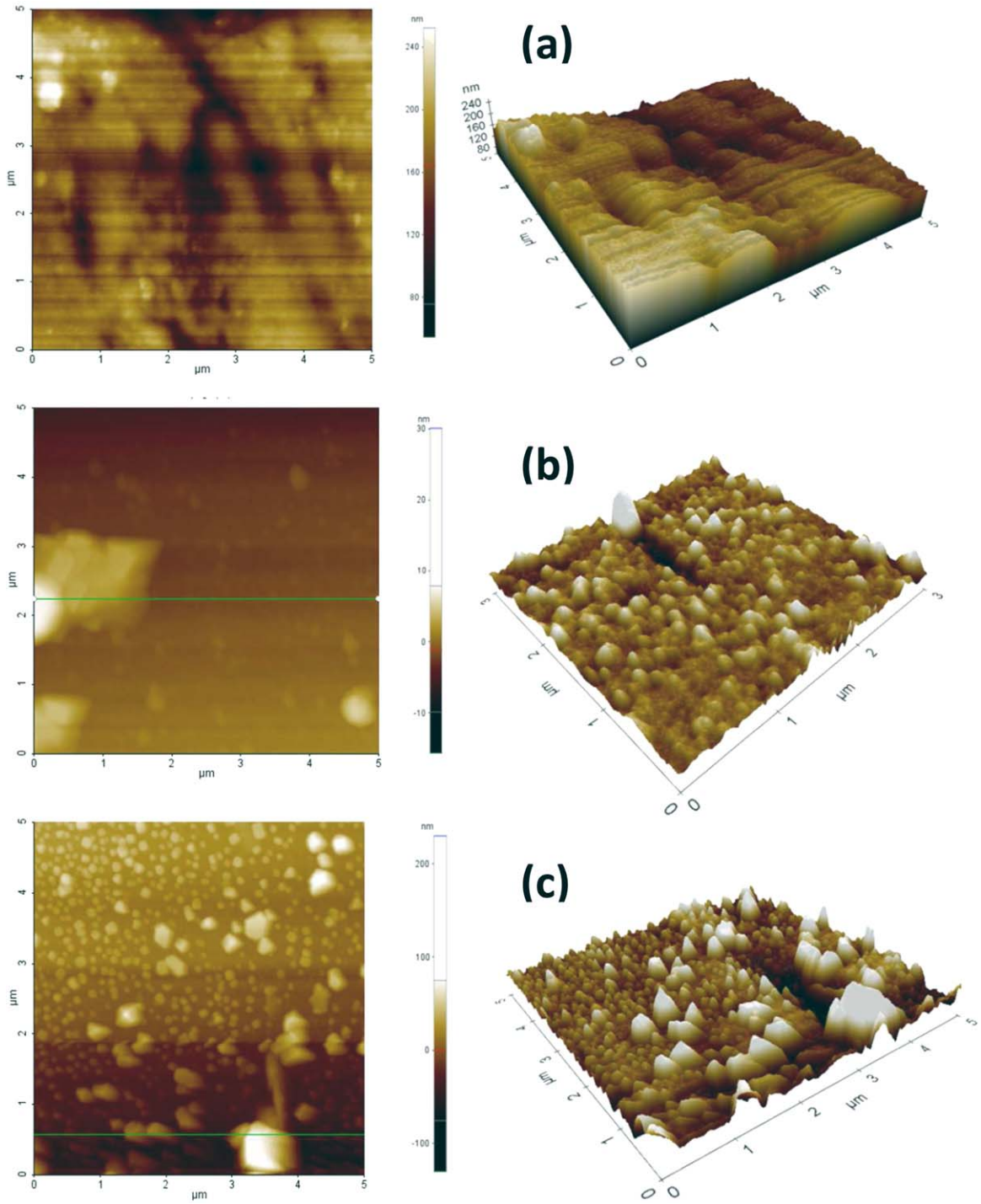

Figure 4. AFM images of PPy:PSS Multilayer films (a) 1 Layer (b) 3 Layers (c) 5 Layers. [Color figure can be viewed in the online issue, which is available at wileyonlinelibrary.com.]

coated on FTO, very smooth and uniform films were obtained. Hence, increasing the number of PPy:PSS deposition resulted in darker polymer films after annealing and this means, more PPy was being coated on the conductive glass. PSS, acting as a dopant for the polymerization of conductive polymers, remains immobilized in the polymer matrix. During the redox process, they show cation-exchange properties because of their large size.[26] By choosing the PSS molecule and the polymerization conditions correctly, stable nanosize colloidal particles of PPy:PSS aggregate can be formed during polymerization.[45] The stabilization against coagulation arises from the coulomb repulsion between the particles, which are due to the surface charge provided by extra sulfonic acid group in PSS.[46] This could provide higher capacity and higher diffusion of ionic species in

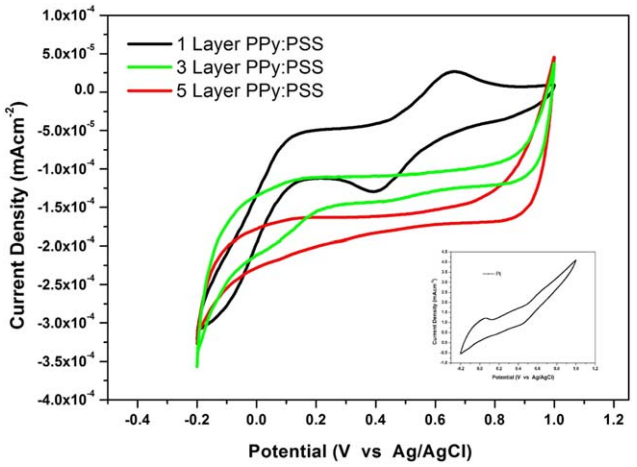

Figure 5. CV curves of the PPy:PSS multilayer films (1, 3, and 5) in 0.1 M H_2SO_4 aqueous solutions recorded at a scan rate of 0.05 V/s. [Color figure can be viewed in the online issue, which is available at wileyonlinelibrary.com.]

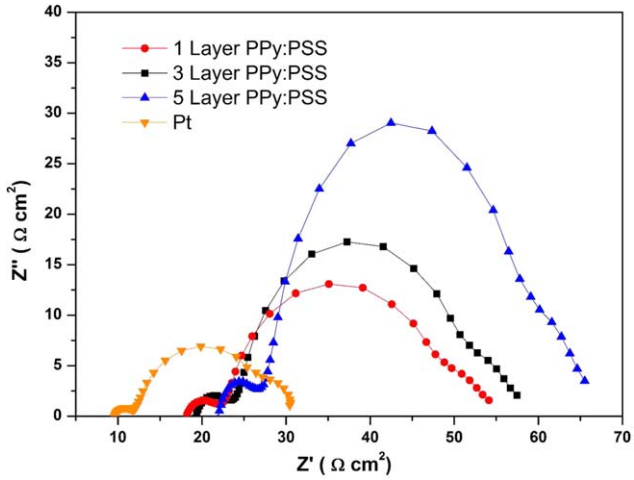

Figure 6. Nyquist plots of DSSCs assembled with PPy:PSS 1, 3, and 5 multilayer films. [Color figure can be viewed in the online issue, which is available at wileyonlinelibrary.com.]

conducting polymer. From AFM images, PPy nanostructured multilayer thin films seem to have rough surfaces with porous structure and high surface area which can have better diffusion efficiency of tri-iodide.[47]

Electrochemical Analysis of PPy:PSS Multilayer Films

The electrocatalytic activity of 15 wt % PSS blended PPy films were analyzed by CV curves. Figure 5 shows the CV curves of 1, 3, and 5 layer PPy:PSS films and Pt CE (inset of Figure 5) with a potential window from −0.2 to 1.0 V at the scan rate of 50mVs^{-1} in 0.1M H_2SO_4 electrolyte solution. The 1 layer PPy:PSS composite film showed a couple of redox peaks at ∼ 0.39 and ∼ 0.65 V, respectively. It is reasonable to indicate that the anodic peak corresponds to the deintercalation of the cation from the PPy:PSS film, and the cathodic peak was caused by the ion intercalation process. Wu *et al.*[21] and Jeon *et al.*[22] achieved faster redox reaction with better catalytic activity of PPy CE, by having larger surface area with PPy nanoparticles in the CE. These well-defined redox peaks as in single layer were absent in the multilayer (3 and 5) PPy:PSS composite films. This may be due to the presence of excess amount of PSS, compared to PPy in the active electrode materials, which could significantly harm the electrocatalytic activity of PPy. To further confirm the better results of single layer film, CV tests were performed up to 20 cycles at the scan rate of 50 mVs^{-1}. It is valuable to note that the structure of CV curves did not change much, with the number of cycles. Further the redox peak currents show good relationship with the cycle number. This tendency of PPy:PSS electrode confirms the good electrochemical stability and the firm attachment of PPy:PSS with the FTO substrate.

The electrochemical characteristics of single and multilayer PPy:PSS CE films were studied through electrochemical impedance spectroscopy (EIS). Figure 6 shows the Nyquist plots obtained for 1, 3, and 5 layers of multilayer PPy:PSS films along with Pt for the frequency range of 0.1 Hz to 1 MHz. The information about resistance of charge transfer (R_{ct}) at the interface between electrode and electrolyte could be drawn from EIS measurements, which is closely related to the electrocatalytic activity of PPy:PSS CE. R_{ct} induces big impact on the photovoltaic parameters such as FF and overall efficiency, hence it reflects the one for the whole device, including both working and counter electrode.[48] Since the TiO_2 photoanode was same for all DSSCs, in addition, the change in R_{ct} can be mainly attributed to the change in PPy:PSS CEs. The calculated R_{ct} values for multilayer PPy:PSS films increased from 5.39 Ω cm^2 for single layer film to 5.68 Ω cm^2 and 6.28 Ω cm^2 for three and five layered films, respectively, which is higher than Pt with 2.14 Ω cm^2. Due to higher R_{ct} values of multilayer CE films, their electrocatalysis were found to be lower. This change in trend agrees well with the CV results along with the performance of DSSCs. Furthermore, lower R_{ct} values of single layer PPy:PSS CE may have contributed to higher Jsc and FF of DSSCs as listed in Table II. For single layer films, the deposition of PPy:PSS nanoparticles were less, leading to better conductivity between the redox couple and CE, which resulted in lesser R_{ct} values and enhanced photovoltaic performance. Wu *et al.*[21] achieved better efficiency than us by using only PPy as CE with small R_{ct} values. Our results were lower due to the presence of excess PSS with SO_3^- groups in PPy matrix of multilayer films causing a higher degree of distortion of the conjugated PPy segments as a result of the steric congestion.[33] Moreover, larger value of R_{ct} induces some perturbation for electrolyte diffusion in the

Table II. Photovoltaic Parameters of the Fabricated DSSCs

PPy:PSS	V_{oc} (mV)	J_{sc} (mA cm^{-2})	FF	Efficiency (%)
1 Layer	630.7	7.2175	0.7154	3.48
3 Layer	635.9	7.1214	0.6397	2.90
5 Layer	604.7	6.5615	0.5054	2.01
Pt	705.4	13.7743	0.6304	6.15

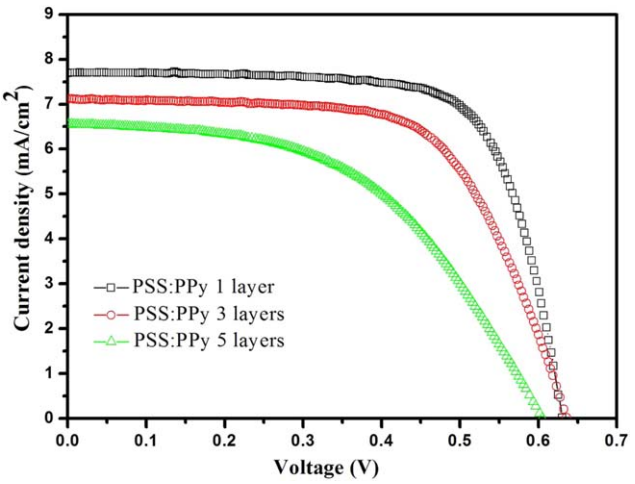

Figure 7. Photocurrent density-Photovoltage (J-V) curves obtained under simulated solar irradiation of AM 1.5 G (100 Mw/cm^2) for the DSSCs having the TiO2/N719/Iodolyte configuration integrated with PPy:PSS nanocomposite based spin coated multilayer C.E. [Color figure can be viewed in the online issue, which is available at wileyonlinelibrary.com.]

multilayer PPy:PSS films, which greatly influenced their impedance behavior. Higher wt % of PSS not only dispersed in PPy matrix, but tends to aggregate on the surface of PPy as seen in the HRTEM image. This could be a possible hindrance between the PPy and the electrolyte. The Ohmic serial resistance (R_s) of PPy:PSS (1, 3, and 5 layered) films are 17.4, 18.7, and 21.5 Ω cm^2, respectively, which is higher than Pt with 9.5 Ω cm^2. The larger R_s of PPy:PSS electrodes is attributed to, the lower electrical conductivity of the films than Pt,[48] which affected the electrocatalytic activity of PPy:PSS films leading to lower photovoltaic efficiencies of DSSCs.

DSSCs Performance

The photoelectric performance of the DSSCs was evaluated with the photocurrent density-photo voltage (J-V) curves for PPy:PSS based CEs, which is shown in Figure 7 and the photovoltaic parameters are listed in Table II. The open circuit voltage (V_{oc}) of all samples is similar, indicating that the value of V_{oc} is not affected by the multilayer films. The energy conversion efficiencies of DSSCs using 1, 3, and 5 multilayers of PPy:PSS as CEs are 3.48, 2.90, and 2.01%, respectively. Although the standard DSSC with Pt as the CE has better cell efficiency under the same measurement conditions, the variable elementary defects in the PPy:PSS can trap the electrons and lower the conductivity of the thin film showing relatively lower performance for multilayer films. This may be due to the formation of microporous structures indicating some disintegrable components released from multilayer films.[49] For multilayer PPy:PSS films, more number of PSS incorporated in to the PPy, will induce some unbounded PPy chains which may prevent transferring electrons between bounded PPy chains. This leads to the decrease in catalytic activity towards the reduction of I_3 in to $\bar{I}$ ions and to regenerate the oxidized dye after the electron injection process and is in accordance with the CV results. As a consequence, the overall energy conversion efficiency of DSSCs was deteriorating with the increase in multilayers of PPy:PSS. The incorporation of higher surfactant PSS in to PPy can decrease the electrical conductivity of PPy which is due to the presence of bulky and hydrophobic component.[31] Hence, excess dopant anion needs to be removed from the polymer matrix, to improve the conductivity of PPy nanoparticles. Unfortunately, for PPy the acidic dopant is hard to be removed from the polymer matrix. This is because the dopant anions have greater affinity to the PPy chain and poor inaccessibility in the polymer matrix.[35] According to Jeon *et al.*,[22] when PPy CE was exposed to HCl vapors for longer time, due to over-oxidation the DSSCs efficiency decreased. We have used HCl in the reaction mixture, and during polymerization the over-oxidation of PPy might have affected the performance of PPy:PSS CE in DSSCs. The J-V curves of DSSCs for 3 and 5 PPy:PSS multilayer films exhibits less squareness and lower FF values of 0.50 and 0.639, respectively, which is lower than Pt CE. This is an indication of higher R_{ct} developed in multilayer films and is in accordance with the EIS values which will depress the electron transport, resulting in poor solar cell performance.[49] Although the DSSCs are fabricated with same FTO glass, TiO_2 films and electrolyte, the different CE will have major influence on different DSSCs impedances. Hence the reduction of cell efficiencies is due to the increase in the impedance for the multilayer films as reported by Khamsone *et al.*[50] Moreover, the unbounded polypyrole chains and larger grain size aggregate of multilayer layer films are also possible factors which are responsible for lower efficiency.[51] The inference we have drawn with the PPy multilayer films prepared with 15 wt % of PSS is that, the wide range of PPy nanoparticles in which the anionic surfactants serving as counterions for the polymer chains, disrupt the spherical structure of polypyrrole permanently. Thus the PPy upon having multilayer coating did not have effective interfacial area in our case, and did not improve the porosity of the film for better DSSC performance. It is noteworthy that the device using the PPy:PSS of single bilayer, as CE showed a higher FF. This implies that, the enhancement of power conversion efficiency can be achieved by applying the conducting polymer as counter electrode. The future work is intended to have a salt treatment with different molarity on the multilayer films which could possibly improve the conductivity of the polypyrrole and the photovoltaic parameters of the DSSCs.

Conclusions

Highly water dispersible and processable polypyrrole nanocolloidal particles were synthesized with 15 wt % of PSS by chemical oxidative polymerization method. Spin-coated multilayer films were deployed as CE for Pt free DSSCs. HR-TEM images showed uniform distribution of PPy nanoparticles with diameter in the range 100 to 500 nm. The higher doping level of PPy with PSS was confirmed by the increase in S/N value of 0.65 when compared to undoped PPy. The surface roughness of multilayer films increased with the number of layers and more number of particles were self-assembled in five layer thin films. Highest energy conversion efficiency for PPy synthesized with 15 wt % of PSS based CE is 3.48%, for one layer PPy:PSS. The performance of DSSCs decreased with the increase in the thickness and roughness of multilayer films to 2.90%, 2.01% for

three layer and five layers. This is attributed to incorporation of higher surfactant PSS in to PPy, decreasing the electrical conductivity of PPy which is due to the presence of bulky and hydrophobic component. The electrocatalytic activity of one layer PPy:PSS films were better than multilayer films. Electrochemical stability for all the single and multilayer films were good, which confirmed the firm attachment of PPy:PSS on the FTO substrate. The higher charge transfer resistance between the multilayer films and electrolyte interface also depressed the electron transport and affected the solar cell performance. Though the dopant anions have greater affinity to the PPy chain, the device using the PPy:PSS of single bilayer as CE showed a higher FF of 0.7154. The low cost, comparable performance, rapid and simple fabrication methods of PPy:PSS composite modified counter electrode, proved to be a potential alternative to the high-cost Pt as counter electrode in DSSC.

REFERENCES

1. O'regan, B.; Grätzel, M. *Nature* **1991**, *353*, 737.
2. Crossland, E. J. W.; Noel, N.; Sivaram, V.; Leijtens, T.; Webber, J. A. A.; Snaith, H. J. *Nature* **2013**, *495*, 215.
3. Hodes, G.; Cahen, D. *Acc. Chem. Res.* **2012**, *45*, 705.
4. Han, J.; Kim, H.; Kim, D. Y.; Jo, S. M.; Jang, S. Y. *Nano* **2010**, *4*, 3503.
5. Thomas, S.; Deepak, T. G.; Anjusree, G. S.; Arun, T. A.; Nair, S. V.; Nair, A. S. *J. Mater. Chem. A* **2014**, *2*, 4474.
6. Olsena, E.; Hagen, G; Lindquistc, S. E. ; *Sol, Energy Mater. Sol. Cells.* **2000**, *63*, 267.
7. Dong, P.; Pint, C. L.; Hainey, M.; Mirri, F.; Zhan, Y.; Zhang, J.; Pasquali, M.; Hauge, R. H.; Verduzco, R.; Jiang, M.; Lin, H.; Lou, J. *Appl. Mater. Interfaces* **2011**, *3*, 3157.
8. Kang, D. Y.; Lee, Y.; Cho, C. Y.; Moon, J. H. *Langmuir* **2012**, *28*, 7033.
9. Wu, M.; Lin, X.; Wang, Y.; Wang, L.; Guo, W.; Qi, D.; Peng, X.; Hagfeldt, A.; Grätzel, M.; Ma, T. *J. Am. Chem. Soc.* **2012**, *134*, 3419.
10. Gong, F.; Wang, H.; Xu, X.; Zhou, G.; Wang, Z. S. *J. Am. Chem. Soc.* **2012**, *134*, 10953.
11. Zhang, L.; Liu, J.; Xiao, H.; Liu, D.; Qin, Y.; Wu, H.; Li, H.; Du, H.; Hou, W. *Chem. Eng. J.* **2014**, *250*, 1.
12. Balamurugan, J.; Thangamuthu, R.; Pandurangan, A.; Jayachandran, M. *J. Power Sources* **2013**, *225*, 364.
13. Tian, H.; Yu, Z.; Hagfeldt, A.; Kloo, L.; Sun, L. *J. Am. Chem. Soc.* **2011**, *133*, 9413.
14. Kim, Y.; Lee, J.; Yeom, M. S.; Shin, J. W.; Kim, H.; Cui, Y.; Kysar, J. W.; Hone, J.; Jung, Y.; Jeon, S.; Han, S. M. *Nat. Commun.* **2013**, *4*, 2114.
15. Wang, S.; Lu, S.; Li, X.; Zhang, X.; He, S.; He, T. *J. Power Sources* **2013**, *242*, 438.
16. Li, C.; Bai, H.; Shi, G. *Chem. Soc. Rev.* **2009**, *38*, 2397.
17. Wang, L. X.; Li, X. G.; Yang, Y. L. *React. Funct. Polym.* **2001**, *47*, 125.
18. Zhanga, X.; Wanga, S.; Lua, S.; Sua, J.; He, T. J. *Power Sources* **2014**, *246*, 491.
19. Stejskal, J. J. *Polym. Mater.* **2001**, *18*, 225.
20. Omastova, M.; Trchova, M.; Pionteck, J.; Prokes, J.; Stejskal, J. *Synth. Met.* **2004**, *143*, 153.
21. Wu, J.; Li, Q.; Fan, L.; Lan, Z.; Li, P.; Lin, J.; Hao, S. *J. Power Sources* **2008**, *181*, 172.
22. Jeon, S. S.; Kim, C.; Ko, J.; Im, S. S. *J Mater. Chem.* **2011**, *21*, 8146.
23. Nishio, K.; Fujimoto, M.; Ando, O.; Ono, H.; Murayama, T. *J. Appl. Electrochem.* **1996**, *26*, 425.
24. Oh, E. J.; Jang, K. S.; MacDiarmid, A. G. *Synth. Met.* **2001**, *125*, 267.
25. Qi, Z.; Pickup, P. G. *Chem. Mater.* **1997**, *9*, 2934.
26. Qu, L.; Shi, G. J. *Polym. Sci., Part A: Polym. Chem.* **2004**, *42*, 3170.
27. Luo, Q.; Li, X.; Wang, D.; Wang, Y.; An, J. *J. Mater. Sci.* **2011**, *46*, 1646.
28. TamilSelvan, S.; Hayakawa, T.; Nogami, M.; Moller, M. *J. Phys. Chem B.* **1999**, *103*, 7441.
29. Wu, T. M.; Chang, H. L.; Lin, Y. W. *Compos. Sci. Technol.* **2009**, *69*, 639.
30. Joo, J.; Lee, J. K.; Lee, S. Y.; Jang, K. S.; Oh, E. J.; Epstein, A. *J. Macromol.* **2000**, *33*, 5131.
31. Wu, T. M.; Chang, H. L.; Lin, Y. W. *Polym. Int.* **2009**, *58*, 1065.
32. Omastova, M.; Trchova, M.; Kovarova, J.; Stejskal, J. *Synth. Met.* **2003**, *138*, 447.
33. Chen, N.; Hong, L. *Eur. Polym. J.* **2001**, *37*, 1027.
34. Zhang, X.; Zhang, J.; Song, W.; Liu, Z. *J. Phys. Chem. B* **2006**, *110*, 1158.
35. Wang, H.; Lin, T.; Kaynak, A. *Synth. Met.* **2005**, *151*, 136.
36. Wang, G.; Xing, W.; Zhuo, S. *J. Power Sources* **2009**, *194*, 568.
37. Jia, R.; Chen, J.; Zhao, J.; Zheng, J.; Song, C.; Li, L.; Zhu, Z. *J. Mater. Chem.* **2010**, *20*, 10829.
38. Manoharan, D.; Chandrasekaran, J.; Maruthamuthu, S.; Jayamurugan, P. *Mater. Sci. Semicond. Process* **2015**, *34*, 382.
39. Gao, C.; Leporatti, S.; Moya, S.; Donath, E.; Mohwald, H. *Chem. Eur. J.* **2003**, *9*, 915.
40. Pingree, L. S. C.; MacLeod, B. A.; Ginger, D. S. *J. Phys. Chem. C* **2008**, *112*, 7922.
41. Huang, J.; Miller, P. F.; Wilson, J. S.; de Mello, J. J.; de Mello, J. C.; Bradley, D. D. C. *Adv. Funct. Mater.* **2005**, *15*, 290.
42. Kymakis, E.; Koudoumas, E.; Franghiadakis, I.; Amaratunga, G. A. J. *J. Phys. D: Appl. Phys.* **2006**, *39*, 1058.
43. Sun, L.; Wang, J.; Butt, H. J.; Bonaccurso, E. *Small* **2011**, *7*, 950.
44. Bae, W. J.; Kim, K. H.; Jo, W. H. *Macromolecules* **2005**, *38*, 1044.
45. Zhang, X.; Zhang, J.; Liu, Z.; Robinson, C. *Chem. Commun.* **2004**, 1852.

46. Greco, F.; Zucca, A.; Taccola, S.; Menciassi, A.; Fujie, T.; Haniuda, H.; Takeoka, S.; Dario, P.; Mattoli, V. *Soft Matter* **2011**, *7*, 10642.

47. Bu, C.; Tai, Q.; Liu, Y.; Guo, S.; Zhao, X. Z. *J. Power Sources* **2013**, *221*, 78.

48. Lu, S.; Wang, S.; Han, R.; Feng, T.; Guo, L.; Zhang, X.; Liu, D.; He, T. *J. Mater. Chem. A* **2014**, *2*, 12805.

49. Gui, Z.; Qian, J.; Zhao, Q.; Ji, Y.; Liu, Y.; Liu, T.; An, Q. *Colloids Surf. A: Physicochem. Eng. Aspects* **2011**, *380*, 270.

50. Keothongkham, K.; Pimanpang, S.; Maiaugree, W.; Saekow, S.; Jarernboon, W.; Amornkitbamrung, V. *Int. J. Photoenergy* **2012**, *2012*, 7. pages.

51. Halme, J.; Vahermaa, P.; Miettunen, K.; Lund, P. *Adv. Mater.* **2010**, *22*, E210.